

# A comprehensive review of earthquake-induced building damage detection with remote sensing techniques



Laigen Dong<sup>a</sup>, Jie Shan<sup>b,a,\*</sup>

<sup>a</sup> School of Remote Sensing and Information Engineering, Wuhan University, 129 Luoyu Rd., 430079 Wuhan, China

<sup>b</sup> School of Civil Engineering, Purdue University, West Lafayette, IN 47907, USA

## ARTICLE INFO

### Article history:

Received 6 January 2013  
Received in revised form 1 April 2013  
Accepted 28 June 2013  
Available online 7 August 2013

### Keywords:

Earthquakes  
Building damage detection  
Remote sensing

## ABSTRACT

Earthquakes are among the most catastrophic natural disasters to affect mankind. One of the critical problems after an earthquake is building damage assessment. The area, amount, rate, and type of the damage are essential information for rescue, humanitarian and reconstruction operations in the disaster area. Remote sensing techniques play an important role in obtaining building damage information because of their non-contact, low cost, wide field of view, and fast response capacities. Now that more and diverse types of remote sensing data become available, various methods are designed and reported for building damage assessment. This paper provides a comprehensive review of these methods in two categories: multi-temporal techniques that evaluate the changes between the pre- and post-event data and mono-temporal techniques that interpret only the post-event data. Both categories of methods are discussed and evaluated in detail in terms of the type of remote sensing data utilized, including optical, LiDAR and SAR data. Performances of the methods and future efforts are drawn from this extensive evaluation.

© 2013 International Society for Photogrammetry and Remote Sensing, Inc. (ISPRS) Published by Elsevier B.V. All rights reserved.

## Contents

1. Introduction	86
2. Metrics and methodological overview for building damage detection	87
3. Building damage detection using both pre- and post-event data	89
3.1. Optical data	89
3.1.1. Visual interpretation	89
3.1.2. Image enhancement	89
3.1.3. Post classification comparison	90
3.1.4. Other methods	90
3.2. SAR data	91
3.2.1. Amplitude information	91
3.2.2. Phase information	91
3.2.3. Combination of amplitude and phase information	91
3.3. LiDAR data	91
3.4. Optical and SAR data	92
3.5. Ancillary data	92
4. Building damage detection using only post-event data	93
4.1. Optical data	93
4.1.1. Visual interpretation	93
4.1.2. Edge and textures	93
4.1.3. Spectra and others	93
4.2. SAR data	94

\* Corresponding author at: School of Civil Engineering, Purdue University, West Lafayette, IN 47907, USA.

E-mail address: [jshan@ecn.purdue.edu](mailto:jshan@ecn.purdue.edu) (J. Shan).

4.3. LiDAR data .....	94
4.4. Optical and LiDAR data .....	94
4.5. Ancillary data .....	95
5. Conclusion .....	96
Acknowledgement .....	96
References .....	96

## 1. Introduction

Earthquakes are some of the most catastrophic natural disasters to affect mankind. More than a million earthquakes occur worldwide every year, which equates to roughly two earthquakes per minute. During the period of 2001–2011 alone, disasters have caused more than 780,000 deaths, with earthquakes accounting for nearly 60% of all disaster-related mortality (Bartels and VanRooyen, 2011). The threat of earthquakes will probably increase because of global urbanization, and thus millions of people are exposed to earthquakes. Although humans cannot prevent earthquakes, we can change the way we respond to them. Fortunately, remote sensing techniques, both spaceborne and airborne, can make a very effective contribution (Voigt et al., 2007). For instance, thermal infrared imagery can be used for earthquake prediction (Tronin et al., 2002; Ouzounov et al., 2006; Joyce et al., 2009); InSAR (Interferometric Synthetic Aperture Radar) for measuring Earth's surface deformation (Gabriel et al., 1989; Massonnet et al., 1993); optical, SAR, LiDAR (Light Detection And Ranging) data can also be used for building damage assessment (Ehrlich et al., 2009; Corbane et al., 2011). This paper is focused on the application of remote sensing data for building damage assessment, especially in the response and recovery phases. In 1972, several American scientists used six remote sensing images to ascertain the causes of the 1964 Alaska earthquake (Duan et al., 2010), which was probably the inaugural application of remote sensing in the seismic field. Subsequently, many tentative experiments on the detection of earthquake-induced building damage were conducted; and researchers have gained valuable insights

through these studies conducted all over the world. Table 1 summarizes many of the severe earthquakes and the published research available pertaining to them.

Earthquake-induced building damage is one of the most critical threats to cities. The area and amount of damage, the rate of collapsed buildings, the grade of damage in the affected area, and the type of damage incurred by each building are essential information for successful rescue and reconstruction in disaster areas (Schweier and Markus, 2006). To achieve this objective, the spatial resolution of the data needs to be high enough to discriminate between buildings and other features. Most of the data used in the representative research is at high resolution and can be classified into four categories: (1) optical, (2) SAR, (3) LiDAR, and (4) ancillary data. The ancillary data include maps produced from GIS data acquired by remote sensing and in situ building damage assessment. Classified by their acquisition platform and sensor types, Table 2 shows some data at finer than 10 m spatial resolution that is suitable for detection of earthquake-damaged buildings. Among the available data, optical images can be used to extract various properties of buildings, such as gray scale, spectra, texture, shape, morphological features (Gamba and Casciati, 1998; Rathje et al., 2005a; Guo et al., 2009), whereas building height and volume information can be derived from digital elevation model (DEM) or stereoscopic measurement (Turker and Cetinkaya, 2005; Rezaeian and Gruen, 2007; Tong et al., 2012). It should be noted that because of its reasonable cost, large coverage, and fast data acquisition capability, a huge amount of remotely-sensed data maybe available today for one incident. For instance, after the Haiti earthquake, the unprecedented amount and unusually diverse types of remotely-sensed

**Table 1**  
Selected severe earthquakes and reported studies since 1976.

Earthquakes	References
1976 Tangshan, China	Liu et al. (2004)
1980 Santomena, Italy	Gamba and Casciati (1998)
1995 Kobe, Japan	Ogawa and Yamazaki (2000), Yonezawa and Takeuchi (2001), Yonezawa et al. (2002), Ito et al. (2000); Mitomi et al. (2002), Matsuoka and Yamazaki (2004)
1999 Izmit, Turkey	Turker and San (2003, 2004), Turker and Cetinkaya (2005), Guler and Turker (2004), Sumer and Turker (2006), Stramondo et al. (2006), and Brunner et al. (2010)
1999 Kocaeli, Turkey	Matsuoka and Yamazaki (2000), Sumer and Turker (2006), and Rasika et al. (2006)
1999 Nantou, Taiwan	Zhang et al. (2003)
2001 Gujarat, India	Yusuf et al. (2001), Saito et al. (2004), and Liu et al. (2004)
2003 Bam, Iran	Sakamoto et al. (2004), Adams et al. (2005), Saito and Spence (2005), Kohiyama and Yamazaki (2005), Yamazaki et al. (2005), Yamazaki and Matsuoka (2007), Rathje et al. (2005a, 2005b), Gusella et al. (2005), Huyck et al. (2005), Matsuoka and Yamazaki (2005), Vu et al. (2005), Stramondo et al. (2006), Hoffmann (2007), Gamba et al. (2007a), Arciniegas et al. (2007), Chesnel et al. (2007), Rezaeian and Gruen (2007), Samadzadegan and Rastiveisi (2008), Chini et al. (2009), Rezaeian (2010), Brunner et al. (2010), and Bignami et al. (2011)
2003 Boumerdes, Algeria	Vu et al. (2004), Yamazaki et al. (2004), Bitelli et al. (2004), Trianni and Gamba (2008)
2004 Darfur, Sudan	Tomowski et al. (2010)
2004 Indonesia	Chini et al. (2008)
2005 Kashmir, Pakistan	Chini et al. (2011)
2006 Mid Java, Indonesia	Matsuoka and Yamazaki (2006), Miura et al. (2007), Yamazaki et al. (2007), Brunner et al. (2010), Kerle (2010)
2007 Peru	Trianni and Gamba (2008)
2008 Wenchuan, China	Li et al. (2009), Guo et al. (2009), Wang et al. (2009), Wang and Jin (2009), Liu et al. (2010), Vu and Ban (2010), Duan et al. (2010), Balz and Liao (2010), Pan and Tang (2010), Dong et al. (2011), Tong et al. (2012), Ma and Qin (2012)
2009 L'Aquila, Italy	Dell'Acqua et al. (2011), Guida et al. (2010), Polli et al. (2010), Cossu et al. (2012)
2010 Haiti	Polli et al. (2010), Yu et al. (2010), Dell'Acqua and Polli (2011), Gerke and Kerle (2011), Malinverni (2011), Hussain et al. (2011), Miura et al. (2011), Uprety and Yamazaki (2012), and Wang and Jin (2012)
2010 Yushu, China	Ma and Qin (2012)
2011 Tohoku, Japan	Satake et al. (2012) and Liu et al. (2012)

data such as optical, SAR, and LiDAR from both spaceborne and air-borne sensors was freely supplied by the humanitarian organizations, governmental agencies, and commercial companies (Corbane et al., 2011).

A review of the literature revealed that little research has been done on a comparative evaluation of various building damage detection methods. This paper intends to fill this gap by providing a thorough review of recent progress in building damage detection. The performance of different remote sensing methods is also examined to expose their strengths and limitations. The remainder of the paper is structured as follows. Section 2 introduces the metrics for building damage assessment and presents an overview for related studies. The group of methods using both pre- and post-event data is discussed in Section 3 in terms of the type of data applied. Section 4 follows a similar format but focuses on the group of methods using only post-event data. Section 5 summarizes the

reported performances of the two groups of methods in building damage detection and draws thereafter our concluding remarks on the findings and future efforts.

## 2. Metrics and methodological overview for building damage detection

Building damage is often measured by grades (Saito and Spence, 2005; Yamazaki et al., 2005), which need to be clarified for our review. At a resolution of 10 m or coarser, earthquake-induced building damage can only be detected and classified into several basic damage grades at the (building) block level. Moving to meter and sub-meter resolutions, detecting building level damage and precise damage grading become possible. Damage classification and grading for different types of buildings has thus been studied and

**Table 2**  
Summary of remote sensing data suitable for building damage assessment.

Data type	Acquisition platform	Sensor	Spatial Resolution (nadir)[m]	Revisit capability	Launch date		
Optical	Air borne	Airplane, unmanned aerial vehicle (UAV), balloon	ADS, DMC, UCD, SWDC	ca 0.1	Mobilized to order	Since 1972	
	Space borne	QuickBird	Panchromatic	0.6	1.5–3 days	October 2001	
		Worldview-1	Panchromatic	2.4	1.7 days	September 2007	
		Worldview-2	Panchromatic	0.46	1.1 days	October 2009	
		IKONOS	Panchromatic	Multispectral	1.85	1.5–3 days	September 1999
				Multispectral	4		
		RapidEye	Multispectral	5	1 day	Aug.ust2008	
		ALOS	PRISM	AVNIR	4	2 days	January 2006
				AVNIR	10	2–3 days	September 2008
		GeoEye-1	Panchromatic	0.41	2–3 days		
		SPOT-4	Panchromatic	Multispectral		1.65	2–3 days
				Multispectral	10		
		SPOT-5	Panchromatic	5	1 day	September 2012	
		SPOT-6	Multispectral	6	1 day	December 2011	
		Pleiades-1	Panchromatic	0.5	1 day	July 2007	
		KOMPSAT-2	Panchromatic	Multispectral	2	2–3 days	May 2004
				Multispectral	4		
		Formosat-2	Panchromatic	2	1 day	July 2003	
		OrbView-3	Panchromatic	Multispectral	8	3 days	December 2000
				Multispectral	1		
EROS-A	Multispectral	4	5 days	April 2006			
EROS-B	Panchromatic	1.9	5 days	October 2003			
IRS-P6 (Resourcesat-1)	Multispectral	5.8	5 days	May 2005			
IRS-P5 (Cartosat-1)	Panchromatic	2.5	5 days	Since 1972			
SAR	Air borne	Airplane, UAV	MEMPHIS,	ca 0.1	Mobilized to order	Since 1972	
	Space borne	SAOCOM		10	16 days	2003	
		ALOS	PALSAR	10	2 days	January 2006	
		Radarsat-1	Fine	8	24 days	November 1995	
		Radarsat-2	Ultra-fine	Fine	3	24 days	December 2007
				Fine	8		
		Cosmo-Skymed	Spotlight	Stripmap	8	1.5 days	June 2007
				Stripmap	1		
TerraSAR-X	Spotlight	Stripmap	3	2.5 days	June 2007		
		Stripmap	1				
LiDAR	Ground Aerial	Van Airplane, UAV	Lynx Mobile Mapper ALTM Orion, ALS70, LMS-S560-A, Harrier 68i, Falcon	<0.1 ca 0.1	Mobilized to order	Since 1986	

proposed. For example, the European Macroseismic Scale 1998 (EMS98), as shown in Table 3, including five damage grades (slight damage, moderate damage, heavy damage, very heavy damage, and destruction) is commonly used for damage classification of masonry and reinforced buildings (Grunthal, 1998). Wood frame buildings have four damage grades (no damage, moderate damage, heavy damage, and major damage) as proposed by the Japanese Prime Minister's Office (Kawai, 1995). Okada and Takai (2000) proposed a damage index which was a damage classification catalog for various kinds of buildings. The application of LiDAR data, airborne oblique images, and multi-perspective images makes it possible to detect the specific damage type for individual damaged buildings. As the existing building damage catalog did not meet the requirements for this purpose, Schweier and Markus (2006) considered some typical damage types, such as inclined plane, multi-layer collapse, outspread multi-layer collapse, pancake collapse with different stories, heap of debris on un-collapsed stories, heap of debris, overturn collapse separated, inclination, and overhanging elements.


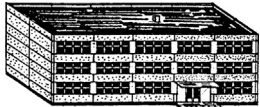





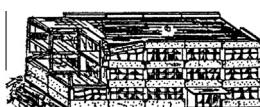


Much work has been done to figure out the relationship between the damage grades (e.g., from EMS98) and building appearance in remote sensing data, which may be different between optical and SAR data (Chini et al., 2009), and vary for different regions of the world (Rathje et al., 2005a). Bignami et al. (2011) investigated the sensitivity of the textural features of objects (contrast, dissimilarity, entropy, and homogeneity) to building damage grades from EMS98 using a pair of QuickBird images acquired before and after the Bam earthquake and ground truth data. No significant sensitivity was found that allows for an operational use of this approach. Wang et al. (2009) analyzed the characteristics of damaged buildings in high resolution airborne SAR images in combination with optical images for the Wenchuan earthquake. They found that damaged buildings could be identified in high resolution SAR images in proper imaging conditions. Dell'Acqua et al.

(2011) studied the relationship between the block-averaged damage-induced changes in radar reflectivity patterns and the changes in texture statistics to investigate damage assessment based on only post-event COSMO/SkyMed data. Pan and Tang (2010) investigated the relationship between building damage grade and differences of backscattered intensity in pre- and post-event SAR images in case of the Wenchuan earthquake, and classified the buildings into three categories: extremely destroyed, moderately destroyed and slightly destroyed. Cossu et al. (2012) investigated the relationship between some textural features and the damage by using SAR images of different resolutions.

In general, heavy damage grades such as the totally collapsed category are detectable. Identification of lower damage grades (e.g., equal to or less than Grade 2 from EMS98) at the building level remains a challenge, even with 0.5 m resolution remote sensing data (Ehrlich et al., 2009; Yamazaki et al., 2005; Kerle, 2010). Thus it is difficult to construct an explicit one-to-one correspondence between the building damage grades from these categories (e.g., EMS98) and their appearances in remote sensing data. As a result, in order to achieve satisfactory outcome in building damage detection, varying damage grading schemes are defined according to the type and quality of the remote sensing data used. Thus, several lower damage grades are aggregated as one grade for building damage classification in practice.

Various methods have been designed for building damage detection. These methods can be basically divided into two groups: (1) methods that detect changes between pre- and post-event data and (2) methods that interpret only post-event data (see Fig. 1). The main differences between these two groups of methods lie in their applicability and quality of the results. Compared to methods using only post-event data, more accurate results can be obtained by those using pre- and post-event data. However, multi-temporal techniques have a major limitation in that many cities, especially in developing countries, do not have pre-event reference data

**Table 3**  
Classification of damage to masonry and reinforced buildings (Taken from EMS98, Grunthal, 1998).

Masonry buildings	Reinforced buildings	Classification of damages
		Grade 1: Negligible to slight damage (no structural damage, slight non-structural damage)
		Grade 2: Moderate damage (slight structural damage, moderate non-structural damage)
		Grade 3: Substantial to heavy damage (moderate structural damage, heavy non-structural damage)
		Grade 4: Very heavy damage (heavy structural damage, very heavy non-structural damage)
		Grade 5: Destruction (very heavy structural damage)

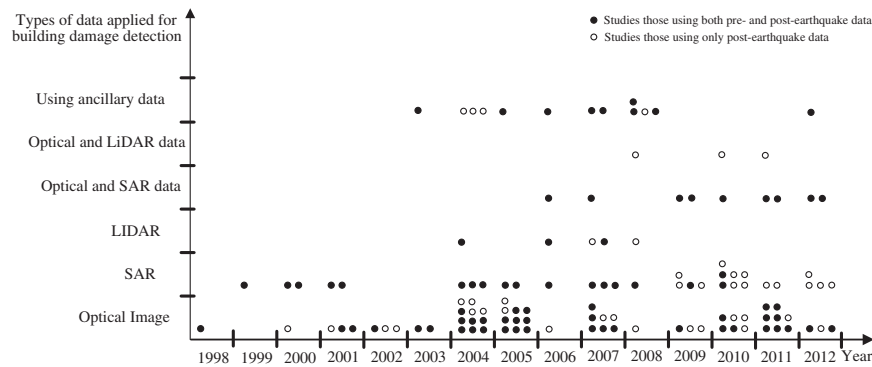


Fig. 1. Selected representative studies since 1998 in terms of data used.

(Li et al., 2011), or do not have a homogeneous pair of pre- and post-event images when data come from the newest very high resolution (VHR) spaceborne radar systems such as COSMO/SkyMed (C/S) and TerraSAR-X, for which the availability of highest resolution data is still scarce (Cossu et al., 2012). Even when pre-event data are available, there can be a problem obtaining reliable and accurate results because of big color and spectral differences between the pre- and post-event data (Kaya et al., 2011). The principal advantage of methods using only post-event data is that building damage detection can be conducted without reference data and is suitable for fast initial building damage evaluation and rapid response; however, the obvious shortcoming of mono-temporal techniques is less satisfactory detection outcome given the difficulty in precisely identifying damage without knowing what existed before the earthquake.

### 3. Building damage detection using both pre- and post-event data

Change detection using both pre- and post-earthquake remote sensing data is a popular method to acquire building damage information. Change detection approaches, including image enhancement and post-classification comparison (Mas, 1999), identify the differences in the state of a building by observing it at different times. The image enhancement method deploys mathematical operations to combine different temporal images such as subtraction of bands, rationing, and image regression to identify changed areas. Post-classification comparison examines different temporal images after independent classification (Coppin et al., 2004). Methods of the representative studies (see Table 1) using both pre- and post-event data will be discussed below in terms of the type of data utilized.

#### 3.1. Optical data

Optical imagery with spatial resolution finer than one meter can be acquired by both spaceborne and airborne sensors (see Table 2). Some of these sensors have existed for over 10 years and have imaged large parts of Earth. The increased availability of this type of imagery and the frequently updated image archives make VHR optical data well-suited as a pre-event reference data source for building damage detection. Over the past decade, the value of optical remote sensing techniques for citywide building damage assessment has been increasingly recognized.

##### 3.1.1. Visual interpretation

Superimposing the pre- and post-earthquake images exactly (in order to perform automated change detection for two temporal images with totally different imaging parameters) is not easy.

Therefore, visual interpretation of optical images, rather than automated change detection, is widely used in practice for building damage detection. Saito et al. (2004) visually interpreted collapsed buildings using three IKONOS images taken before and after the Gujarat earthquake, and confirmed the quality of the results by ground survey data. Further, Saito and Spence (2005) compared the visual interpretation results from only post-event QuickBird images with those from pre- and post-event images, and revealed that the building damage tended to be underestimated when only post-event images were available. Adams et al. (2005) used a visualization system integrated pre- and post-event QuickBird imagery to direct rescuers to the hardest hit areas and support efficient route planning and progress monitoring in the emergency response phase of the Bam earthquake. By comparing the pre- and post-event QuickBird imagery visually, Yamazaki et al. (2005) classified the damaged buildings caused by the Bam earthquake into four damage grades (EMS98). Comparing the results to field survey data revealed that the pre-event imagery was more helpful in detecting lower damage grades through visual interpretation. Damaged buildings of lower damage grades are difficult to identify when only using post-event data; and the detection rate is lower than those of high damage grades. Generally, good results at the building level can be obtained by visual interpretation as demonstrated in these studies. Unfortunately, visual interpretation is time-consuming, requires trained operators, and generates a heavy workload, making it unsuitable for rapid damage assessment over an extensive area.

##### 3.1.2. Image enhancement

Images acquired before and after an earthquake are co-registered and subtracted to produce a residual image which represents the change between the two temporal datasets. Gamba and Casciati (1998) developed an automatic system for building damage assessment using pre- and near-real-time post-event aerial images. This method is based on shape analysis and perceptual grouping. As compared with the results of visual interpretation, about 70% of the collapsed buildings in two tests can be detected correctly by applying this system. Yusuf et al. (2001) detected damaged urban areas by comparing the brightness values of Landsat-7 panchromatic images acquired before and after the Gujarat earthquake. Ishii et al. (2002) proposed an image differencing algorithm to extract the damaged areas by thresholding the color difference in the same geographical location of the pre- and post-event aerial images. The difficulty of this method is the damage detection in shadowed areas. Zhang et al. (2003) introduced a method based on image structure features. In this method, the damage grade at the block level was worked out by thresholding the differences of the mean gray scale and the mean variance of the pre- and post-event images. Comparison with field survey data revealed that the result was precise and the level of error was

within an acceptable range. Kohiyama and Yamazaki (2005) detected damaged areas after the Bam earthquake using 15 m resolution Terra-ASTER images. In this method, the fluctuation of the digital numbers was modeled as a normal random variable based on pre-event images on a pixel-by-pixel basis. Then, the deviation value of each digital number in a post-event image was evaluated and converted into a confidence level, which indicated the possibility of surface changes induced by the earthquake. As compared with the results from QuickBird imagery, it was hard to identify whether the damage was caused by collapsed buildings or dusty roads in the imagery at this resolution. Sakamoto et al. (2004) introduced a nonlinear mapping method for detecting geographical changes from a pair of QuickBird images automatically. The post-event image was nonlinearly mapped to the pre-event image, and the building damage grade was estimated by computing the distribution of the image matching scores. The detection ratio was 75–90% with 20% false alarms when compared with the field survey results.

The differences between color, spectra, texture, and other features extracted from the registered images can also be used to discriminate damaged and undamaged buildings. Rathje et al. (2005b) proposed a change detection algorithm based on texture features, a correlation coefficient (Haralick et al., 1973) computed between the co-registered pre- and post-event QuickBird images for building damage detection. In this method, the damage distribution was characterized by damage density, which was defined as the percentage of pixels classified as damaged within a 100 by 100 pixel window. Pesaresi et al. (2007) designed a multi-criteria method for automatic detection of damaged buildings in tsunami-affected areas utilizing a combination of radiometric, textural, and morphological features from pre- and post-event QuickBird images. The difficulty of this method is the detection of the damaged buildings without leaving debris on the ground. Tomowski et al. (2010) compared the results from four texture-based change detection approaches applied to QuickBird images. In this study, a comparison of four change detection methods on different texture features showed that the best results could be obtained from using principal component analysis with the “energy” texture feature. Miura et al. (2011) used texture characteristics in the pre-event QuickBird and post-event WorldView-2 images to develop an automatic damage detection method for the Haiti earthquake. As compared with the damage data from the Operational Satellite Applications Programme of United Nations Institute for Training and Research (UNOSAT), 70% of the collapsed buildings were correctly detected, and the results showed that the dissimilarity of the collapsed buildings tended to be larger than that of the non-collapsed buildings.

### 3.1.3. Post classification comparison

Building damage can be detected through a comparison between two independent classification results from pre- and post-event data. The principal advantage of these types of methods is minimizing the effect of radiometric difference between the two data sets. However, the accuracy is totally dependent on the initial classification results. Bitelli et al. (2004) classified building damage into different grades (EMS98) with an object-based change detection approach using pre- and post-event IRS and QuickBird imagery. As compared with the results from pixel-based method, object-based methods are less affected by registration problems. Gusella et al. (2005) proposed an object-based method, based on the statistical characteristics, to quantify collapsed buildings using pre- and post-earthquake QuickBird images. An overall accuracy of 70.5% for damage classification was obtained by this method. Huyck et al. (2005) presented an automated method based on edge dissimilarity for detection of collapsed buildings using QuickBird and IKONOS imagery of the Bam earthquake. The assumption of

this method is that damaged buildings yield a high dissimilarity of edges, as compared with intact buildings, in the post-event imagery. Gamba et al. (2007b) detected damage by comparing the normalized difference vegetation index (NDVI) and linear segments of buildings in pre- and post-event images, the detection rate was above 90%. Yamazaki et al. (2008) detected the debris of collapsed buildings by object-based classification of digital aerial images captured before and after the Off-Mid-Niigata earthquake. Li et al. (2009) presented a method based on combined spectral and spatial information for building damage detection using QuickBird imagery acquired in Dujiangyan area of China after the Wenchuan earthquake. The results showed that the combined use of spectral and spatial features significantly improved the detection rate compared to using spectral information alone. Chini et al. (2011) proposed an automatic method based on morphological profile features for building damage detection using pre- and post-event QuickBird images.

### 3.1.4. Other methods

Other information such as building shadow and roof can be exploited to depict building damage. Based on the relationship between a building and its shadow (Irvin and Mckeown, 1989), Vu et al. (2004) studied how the changes in building structures affect the orientation, shape, and size of their shadows in QuickBird imagery. They found that the differences between shadow lengths in pre- and post-event images can assist detecting collapsed buildings. Further, Iwasaki and Yamazaki (2011) detected mid-story collapsed buildings based on their height change estimated from shadow lengths in pre- and post-event QuickBird images of the Boumerdes earthquake. However, it takes time to measure shadow length manually from images. Chesnel et al. (2007) proposed a method based on analysis of building roofs in pre- and post-event QuickBird images. The correlation between the roof pixels in two temporal images was computed to assess roof damage. The results showed that the critical aspect of change analysis with VHR images is the precise registration of the data; and having a building footprint database available before an earthquake can lead to more reliable results in damage assessment.

Multi-perspective and oblique images are more suitable for making a detailed inventory and collecting building damage information. With depth perception, detection of building's pancake collapse with intact roofs is possible. Turker and Cetinkaya (2005) detected collapsed buildings caused by the Izmit earthquake using DEMs created from pre- and post-earthquake aerial photographs. The differences between the two temporal DEMs were analyzed building-by-building to detect the collapsed ones; a producer's accuracy of 84% was achieved. Features such as average height, volume, and tilting angle formed a normalized digital surface model (DSM), combined with other features such as pixel intensity and segment shape from images, were used to estimate the exact damage grade of each building in Rezaeian and Gruen (2007) and Rezaeian (2010). The buildings were classified as collapsed, partially collapsed, and undamaged. The overall success rate, producer's accuracy, and user's accuracy were 71.4%, 86.5%, and 90.4% respectively. Tong et al. (2012) detected building damage based on 3D geometric changes, especially the building height change, using pre- and post-event IKONOS stereo image pairs. Satisfactory results, both at the building and block levels, were obtained from this method when applied to the Wenchuan earthquake. Gerke and Kerle (2011) classified building damage into three grades at the building level by using multi-perspective airborne oblique images. The application of oblique images can avoid the limitations of traditional image-based methods restricted to vertical views. Malinverni (2011) proposed a building damage detection method based on landscape metrics derived from landscape ecology and implemented in the FRAGSTATS software. The

metrics were applied to the pre- and post-event classified QuickBird and IKONOS images and the damage detection results were obtained at the block level.

### 3.2. SAR data

Besides radar remote sensing's all-weather and all-time data collection capability, its sensitivity to changes in height makes it suitable for mapping urban damage caused by earthquakes. The latest generation of VHR spaceborne SAR sensors like TerraSAR-X and COSMO-SkyMed can reach a resolution of about 1 m and permits analysis of urban areas at the building level. Matsuoka and Yamazaki (1999) and Shinozuka and Loh (2004) studied different appearances of damaged and undamaged areas in SAR images. Stramondo et al. (2008) demonstrated the ability of COSMO-SkyMed imagery to detect the damage in urban areas within a very short time period in the case of the Wenchuan earthquake. Detection of completely destroyed buildings is possible with this type of data, but exact damage grading is still a challenge. Usually, change detection in SAR images is based on a three-step procedure: image despeckling, pixel-by-pixel comparison of two images, and image thresholding (Tzeng et al., 2007). Two basic groups of change detection methods using radar data are based on amplitude and phase information respectively (Liu et al., 2010). In reviewing studies published over the past few years, various building damage detection methods based on pre- and post-event radar images were documented. Three types of methods, based on amplitude, phase, and a combination of both, will be discussed below.

#### 3.2.1. Amplitude information

Using pre- and post-event SAR images, building damage can be detected based on changes in the backscatter coefficient and intensity correlation. Matsuoka and Yamazaki (2004) found that the backscattering coefficients and intensity correlations between the pre- and post-event ERS/SAR images were significantly lower in damaged areas. Subsequently, an automated damaged area detection method based on discriminant analysis was developed. The results showed relatively good agreement with the actual damage distribution determined in a field survey. Further, Matsuoka and Yamazaki (2005) revised this automated method according to the backscattering characteristics in the city of Bam, and used it to map damage from a pair of ENVISAT/ASAR images taken before and after the Bam earthquake. The obtained distribution of severely damaged areas roughly corresponded to those from a field survey and visual interpretation of high resolution optical satellite images. In order to identify buildings with lower damage grade, a method was proposed by Matsuoka and Yamazaki (2006) using time-series ALOS/PALSAR images. They calculated the difference values of the correlation coefficients from pre- and post-event image pairs. This method minimized the effects of signal noise and earth surface temporal changes on building damage estimation. A test was conducted using three images of the Mid Java earthquake. The distribution of the estimated damaged areas was in good agreement with the results obtained by visual interpretation of the VHR optical images as well as the field survey results. Chini et al. (2008) presented two complementary approaches to detect surface changes caused by the 2004 Indonesia earthquake by exploiting the backscattering and correlation coefficients of pre- and post-event ERS and ENVISAT/ASAR images respectively. Their results agreed well with those provided by GPS stations. Wang and Jin (2009) proposed a statistical approach for pre- and post-event ALOS/PALSAR images to assess building damage caused by the Wenchuan earthquake. The results were close to those obtained from aerial photos. Liu et al. (2010) conducted ratio change detection for damage assessment using pre- and post-earthquake ENVISAT/ASAR amplitude images and obtained satisfying results.

Guida et al. (2010) detected destroyed buildings based on changes in the double bounce feature effect using a single pair of pre- and post-event COSMO-SkyMed images taken from the L'Aquila earthquake.

#### 3.2.2. Phase information

Phase information is sensitive to change in building shape due to seismic damage. Ito et al. (2000) presented damage evaluation results for the Kobe earthquake based on coherence imagery that represented the degree of correlation of the phase information. Coherence derived from multi-temporal JERS-1 and ERS/SAR data before and after an earthquake showed temporal decorrelation in damaged regions. Thus, damaged areas can be detected using a set of coherence images. Matsuoka and Yamazaki (2000) investigated the microwave scattering characteristics of areas damaged by the Kocaeli earthquake in pre- and post-event ERS/SAR imagery, and found the degree of coherence was a good index to distinguish slight to moderate damage levels. Yonezawa and Takeuchi (2001) made a damage assessment using the coherence coefficient differences between the pre- and post-event ERS/SAR images. The relation between the decorrelation and the damage grade was investigated. The damage of the buildings changed the backscattering characteristics and led to the decorrelation between data obtained before and after the earthquake. Hoffmann (2007) used the changes of interferometric coherence in pre- and post-event ENVISAT/ASAR images to map the urban damage induced by the Bam earthquake. In this approach, a coherence change index that could be interpreted quantitatively with respect to earthquake damage at the block level was defined. The results agreed closely with independent damage assessments from the IKONOS imagery. Liu et al. (2010) used phase information from pre- and post-event ENVISAT/ASAR images to identify the building damage in the Wenchuan earthquake. After decorrelation analysis, the coherence images obtained by interferometric processing showed that the building damage grade was highly related to the variability index of the coherence coefficient. However, restricted by the source and quality of the SAR data, the quantitative relationship between the coherence coefficients and the damage grades must still be worked out.

#### 3.2.3. Combination of amplitude and phase information

Hybrid methods using a combination of phase and amplitude have been proposed and demonstrated. Using ERS/SAR imagery, Yonezawa et al. (2002) detected the ground surface change due to urban damage using correlation coefficient of single-look intensity data (intensity correlation) and complex correlation coefficient of single-look complex data (coherence). They suggested that the coherence is essential and significantly important to detect damaged urban areas by SAR data, especially when some actual damages do not change the backscattering characteristics. Arciniegas et al. (2007) made a coherence- and amplitude-based analysis of earthquake damage using ENVISAT/ASAR data. They found that between pre- and post-event image pairs, coherence decreased with increasing damage levels, and earthquake damage caused both increases and decreases in amplitude. Their research also revealed that the results from damaged building detection using medium or low resolution SAR images were less conclusive without the aid of additional image data or ground truth information.

### 3.3. LiDAR data

Airborne LiDAR systems allow fast and extensive acquisition of precise height data which can be used for detecting some specific damage types (e.g., pancake collapses) that cannot be identified from 2D images. Since LiDAR is a relatively new technology and many places do not have LiDAR coverage, little research using real

pre- and post-event LiDAR data for building damage detection has been conducted. In order to solve the data availability problem, a CAD-based software tool was developed to generate simulated data for buildings with different damage types. Using this kind of simulated data, Schweier et al. (2004) proposed a building damage analysis approach with three steps: modeling buildings automatically in three dimensions, comparing pre- and post-event models to detect changes, and classifying the changes into different damage types. Rehor (2007) proposed a building damage detection and classification method based on the comparison between planar roof planes from simulated pre-event building models and those from real post-event laser scanning data. In this method, features like volume and height reduction, change of inclination and size can be determined for each pair of corresponding planes after being geometrically overlaid. Then, using these features, building damage was classified according to a “damage catalog” (Schweier and Markus, 2006) with a segment-based fuzzy logic classification method. The main advantage of the application of LiDAR data is that the specific damage type of each building can be identified, which otherwise may not be possible by using optical or SAR imagery.

### 3.4. Optical and SAR data

Although optical data can furnish valuable information about building condition, especially now that spatial resolution has reached finer than 1 meter, the information content of VHR images is affected by differences in acquisition times and changes in the observation angle. On the other hand, changes in amplitude and phase of SAR data have been used successfully for building damage detection because of its all-weather and all-time data collection capability. Comparing optical data and with SAR data directly by the change detection method is difficult because they have entirely different radiometric and physical image formation characteristics (Mercier et al., 2008). Butenuth et al. (2011) proposed a comprehensive infrastructure assessment system for disaster management using the combination of multi-sensor and multi-temporal available data, such as optical imagery, SAR, and DEM. They focused on road damage and obtained the improved results, demonstrating the potential of combined use of multi-source data for damage assessment. Chini et al. (2013) investigated the 2011 Tohoku tsunami inundation and liquefaction by combined using optical, thermal, and SAR data.

The combination of VHR optical and SAR data has been proposed by researchers for building damage detection. Stramondo et al. (2006) explored the combined use of radar and optical satellite imagery for building damage detection in urban areas in the case studies of the Izmit and Bam earthquakes. Pixel-based and object-oriented procedures were tested to extract features from optical and radar data and to compare their damage extraction capabilities. The results showed that the fusion of radar and optical data obtained the highest percentage of correct damaged area classifications compared to SAR or optical data alone. Chini et al. (2009) provided a damage map for individual buildings using morphological features in QuickBird images taken before and after the Bam earthquake. A damage map at the block level was also produced using ENVISAT/ASAR data. They found that the results from the SAR data were improved by using a VHR optical image. Brunner et al. (2010) proposed a method for damage detection at the building level using pre-event QuickBird imagery and post-event TerraSAR-X imagery. In this method, the parameters of a building were estimated from the pre-event optical imagery firstly; then the expected signature of the building in the post-event SAR imagery was predicted based on the building parameters and the acquisition parameters of the SAR imagery. At the end the similarity between the predicted image and the actual SAR image was calculated. Low similarity indicated that the building was destroyed. The overall

accuracy of about 90% was obtained when applying this method to detect the damaged buildings caused by the Wenchuan earthquake. Wang and Jin (2012) proposed an approach based on multi-mutual information for building damage detection using pre-event IKONOS images and post-event COSMO-SkyMed and Radarsat-2 SAR images taken from the Wenchuan earthquake. First, SAR images of rectangular buildings were numerically simulated based on the geometric parameters extracted from optical images. Then, the similarity between the simulated and real SAR images was analyzed and used to determine the building damage grades. About 85% of the damaged buildings were correctly identified. Dell'Acqua et al. (2011) detected building damage by fusing SAR (COSMO/SkyMed) and optical (QuickBird and IKONOS) data from the L'Aquila earthquake. About 81% of the buildings were correctly classified into three damage grades: non-damaged or slightly damaged, low level of damage, and high level of damage. They found that optical data were more suitable for distinguishing between damaged and undamaged areas, while SAR texture features distinguished the extent of the damage at the block scale. Dong et al. (2011) combined the use of GIS data extracted from a pre-event QuickBird image and post-event TerraSAR-X data to detect building damage caused by the Wenchuan earthquake. They confirmed that the results could be improved with the combined use of optical and SAR data. Uprety and Yamazaki (2012) detected damaged buildings after the Haiti earthquake based on the differences in the correlation coefficient and backscattering between pre- and post-event TerraSAR-X images. In this method, building polygons of the sampled areas extracted from the pre-event QuickBird image were used to ascertain the number of damaged buildings. The producer's accuracy for damaged buildings was 66.7%.

### 3.5. Ancillary data

Ancillary data like vector maps are useful for building damage detection with either optical or SAR data. In Turker and San (2003), orthophotos and paper maps generated through field surveys were used to digitize the boundaries of building blocks. When combined with the building boundaries, the damaged areas were detected based on the brightness difference between pre- and post-event SPOT HRV (XS and PAN) images. The overall accuracy was 83%, but the vertically collapsed buildings could not be detected by this method. Samadzadegan and Rastiveisi (2008) proposed a method for automatic detection and classification of damaged buildings caused by the Bam earthquake using integration of QuickBird images and a vector map. In this method, building damage grades were evaluated with a fuzzy inference system by measuring and comparing textural features extracted from pre- and post-event images. The results were classified into four grades at the building level; and the overall accuracy was 74%.

Methods using the combination of SAR images and GIS maps have also been proposed. Mansouri et al. (2007) used four multi-temporal SAR images and ancillary data, such as building height information, for earthquake risk assessment in Tehran, Iran; and a detailed flowchart was produced. Gamba et al. (2007a) proposed a method for rapid earthquake damage detection in urban areas using pre- and post-event ENVISAT ASAR images combined with GIS layers for urban areas and city parcel boundaries. Their study showed that the combination of intensity and phase features enhanced damage pattern recognition. Comparing with an accurate ground truth revealed that it was difficult to map building damage using this kind of SAR data, even using the ancillary data. With the combination of pre- and post-event ALOS/PALSAR data and some ancillary information defining urban blocks, Trianni and Gamba (2008) also discriminated between damaged and undamaged areas at the block level using a statistical analysis of the parameters of the models representing the backscatter intensity



or coherence values for each block. The overall accuracy of the results was improved by introducing the GIS information about the parcel borders in the urban area. Liu et al. (2012) detected damaged buildings based on the changes of backscattering intensity between pre- and post-event TerraSAR-X images. Building level damage was assessed and confirmed by visual interpretation with the help of a GIS map.

#### 4. Building damage detection using only post-event data

The emergence of VHR remote sensing imagery with detailed texture and context information makes it possible to detect building damage based on only post-event data. Much promising work has been conducted in this area. Various properties in spectra, texture, edge, spatial relationship, structure, shape, and shadow damaged buildings in post-event data have been used for damage detection. Although it is difficult to ascertain the exact damage grade of a building by using only post-event VHR data, they are useful for rapid damage assessment during the first response.

##### 4.1. Optical data

While visual interpretation remains to be a basic evaluation approach when using optical data, automatic building damage detection has been largely focused on the combined use of various extracted image features.

###### 4.1.1. Visual interpretation

Visual interpretation based on only post-earthquake optical data is a common practice for damaged building recognition. Ogasawa and Yamazaki (2000) interpreted visually the building damage caused by the Kobe earthquake using single and stereoscopic aerial photographs. As compared with the field data, above 70% overall accuracy of the results could be obtained with either of the two methods. The accuracy of stereoscopic photo-interpretation was higher than that of single photo-interpretation for severely damaged buildings. Yamazaki et al. (2004) visually interpreted the building damage caused by the Boumerdes earthquake using only post-event QuickBird imagery. They classified damaged buildings based on EMS98, and found that the pre-event image was more important for the detection of lower damage grades in visual interpretation.

###### 4.1.2. Edge and textures

Edge can be regarded as a special kind of texture and is widely used as an important feature for building damage detection with only post-event optical imagery. Ishii et al. (2002) proposed a post-event aerial image-based damage detection method. It assumed that the damaged areas are those with a larger number of edges whose orientations follow a uniform distribution in the lightness image. However, there are two difficulties with this method: (1) identification of the damage in shadowed regions and (2) how to set the threshold and parameters automatically. In Mitomi et al. (2002), not only the variance and the predominant direction of edge intensity, but also some statistical textures such as the angular second moment and entropy derived from the co-occurrence matrix of edge intensity were used to determine the difference between damaged and undamaged building areas. Results at moderate accuracy were quickly obtained with aerial images acquired after the Kobe earthquake, but some training data must be selected from the imagery for the classification procedure. Based on the previous work, Vu et al. (2005) developed an automated algorithm to detect damaged buildings caused by the Bam earthquake using post-event IKONOS and QuickBird data. More than 80% of the buildings with damage of Grade 4 and 5 (EMS98)

were classified correctly as compared with the results of visual inspection. Later, Yamazaki et al. (2007) proposed a combined use of edge-based textures, multi-spectral gray tone, and spatial relationships formulated using morphological scale-space. With this approach the debris areas were extracted using edge texture analysis, and the intact buildings were delineated based on scale-space analysis. The overlap between the debris areas detected and the retained building areas implied the grade of building damage. This method was applied to a QuickBird image acquired from the Bam earthquake, and the obtained results agreed well with those of visual detection.

###### 4.1.3. Spectra and others

Spectral and textural information are both commonly used for building damage detection. Liu et al. (2004) proposed an automatic method to detect damaged buildings using the regional structure and texture information found in post-event IKONOS images of the 2001 Bhuj earthquake and aerial photographs of the 1976 Tangshan earthquake. The assumption of this method was that undamaged buildings show homogeneous texture features in images, whereas damaged ones exhibit low gray scale. Therefore, statistical information like the number of independent holes appearing in the thresholded original image can be used to discriminate between the damaged and undamaged buildings. The results were basically consistent with those from visual interpretation. Rasika et al. (2006) detected damaged buildings using multi-scale and multivariate texture-based segmentations considering the texture and color information of oblique aerial images acquired after the Kocaeli earthquake. Sirmacek and Unsalan (2009) presented an automatic building damage detection approach based on the building rooftop and shadow extracted from aerial images. In this method, the damage grade for each building was determined by the ratio between the extracted segments of the rooftop and shadow areas. Duan et al. (2010) detected collapsed buildings with a fragmentation parameter referring to the ratio between the building border pixels and the total building pixels in an image. This approach was based on the idea that if a building is collapsed, it will produce a more complex texture. The results revealed that building collapse rates and fragmentation parameters were strongly correlated. After analyzing the characteristics of buildings with different damage grades and the undamaged buildings in an image, Rathje et al. (2005a) investigated the capability of the distinguishing spectral and textural features for semi-automated building damage detection. The accuracy of damage distribution obtained by applying this method to the post-event QuickBird image of the Bam earthquake reached 91% as compared with the visual identification. Based on the observed spectral reflectance characteristics of surface materials, Miura et al. (2007) identified building damage by classifying post-earthquake QuickBird images. In this method, a damage index was computed from the classified images to evaluate the distribution of building damage; and the results agreed well with those obtained through a field survey. Fukuoka and Koshimura (2011) performed a supervised classification of debris through object-based analysis of post-event aerial photographs acquired after the Tohoku earthquake tsunami disaster and found that the debris could be quantified. Li et al. (2011) proposed an object-oriented method to extract damaged building in 0.5 m resolution aerial images acquired after the Wenchuan earthquake. In this method, image objects obtained by image segmentation were classified as damaged and undamaged by checking various features of objects, including spectral characteristics, texture characteristics, and characteristics of their spatial relations. The results showed that automatic recognition accuracy was better than 90%.

Morphological features have been a focus for building detection research in urban areas for a long time (Pesaresi and Benediktsson,

2001; Benediktsson et al., 2003; Huang and Zhang, 2012). In recent years, these morphological features were studied as a means to detect earthquake-induced damaged buildings. Guo et al. (2009) detected collapsed buildings in post-event aerial images of the Wenchuan earthquake by combining mathematical morphology with an electromagnetic reflection mechanism. More than 90% of the collapsed buildings were identified as compared with the visual interpretation results. Based on the combined use of morphological and spectral features, Ma and Qin (2012) proposed an automatic depiction algorithm for collapsed buildings using aerial images of the Wenchuan and Yushu earthquakes. Both results confirmed by visual interpretation revealed that morphological and texture features were complementary to each other when describing collapsed buildings. Vu and Ban (2010) developed a context-based automated approach for building damage mapping from QuickBird images, in which the context of the damage situation was described by relevant information that included structure, shape, size, spectra, and texture in a morphological scale-space. An overall accuracy of 84% was obtained as compared with the visual interpretation results. This approach requires that the post-event image be acquired very soon after an earthquake because the proposed method relies on debris areas. Kaya et al. (2011) proposed a support vector selection and adaptation method for damage assessment of the 2010 Haiti earthquake using a post-earthquake QuickBird image. With ground truth data, damaged and undamaged samples were selected manually to obtain the reference vectors used in image classification. The obtained damage map agreed well with that by UNOSAT, the Operational Satellite Applications Programme under the United Nations Institute for Training and Research (UNITAR).

#### 4.2. SAR data

Due to its limited archives VHR SAR data is not yet a reliable data source for pre-event reference (Brunner et al., 2010). Therefore, automated building damage detection from only post-event VHR SAR data is desirable at the present time. Unfortunately, it is rather difficult to interpret SAR imagery because of its oblique viewing geometry, occlusion and ambiguity, especially for urban areas. Layover and shadow from high-rise buildings, a great amount of energy from the forward scatter of artificial structures, and frequent double- and multi-bounces can affect the interpretation in urban areas. Despite these difficulties, disaster damage assessment still benefits from VHR SAR data because of their superior resolution and weather-independent surveillance.

Balz and Liao (2010) investigated different characteristics of damaged and undamaged buildings in post-event TerraSAR-X and COSMO-SkyMed images of the Wenchuan earthquake with the help of aerial images. The results confirmed that the corner reflections of collapsed buildings were weaker and less linear than those of undamaged buildings. The appearance of collapsed buildings in high resolution SAR images was drawn, and it was difficult to detect slight damage to buildings. Polli et al. (2010) attempted to build an automated and texture-based classifier for classifying building damage levels using post-event COSMO/SkyMed images of the L'Aquila and Haiti earthquakes. However, the achieved accuracy was not satisfactory; the correlation between a subset of texture measures (i.e., entropy and homogeneity) and the block-averaged damage level was found to be too weak to prefigure any operational use at this stage. Dell'Acqua and Polli (2011) provided some quantitative results at the block level with three damage grades (little or no damage, damaged, and extensively damaged). Brunner et al. (2010) showed that not all building damage types were readily discernible in meter resolution SAR imagery and that damaged buildings could be observed only where parts of the body or the roof had collapsed. In addition, the examples

demonstrated that damaged buildings do not have a distinct scattering signature, while a collapsed building might still produce a signature similar to undamaged structures in a TerraSAR-X image of the Wenchuan earthquake. Further, Brunner et al. (2011) showed that it was possible to classify buildings into several basic damage classes (e.g., heap of debris with planes or heap of debris with vertical elements) using a set of decimeter resolution airborne SAR images acquired from a village after an earthquake. Satake et al. (2012) investigated the damaged areas in 0.3 m resolution airborne SAR images acquired immediately after the Tohoku earthquake and found that it was possible to estimate the volume of a pile of debris. However, few of their results have been reported publicly at this time. Taking the optical images as a benchmark, Chini et al. (2012) attempted to optimally exploit the potential of SAR for interpretation of flooded areas using COSMO-SkyMed data after the 2011 Japan Tsunami.

#### 4.3. LiDAR data

It is not a common practice to obtain laser scanning data right after a disaster only for the purpose of building damage detection. Therefore, methods with post-event LiDAR data alone have rarely been studied. Two institutions: the Institute of Photogrammetry and Remote Sensing (Karlsruhe University, Germany) and the MAP-PAGE team (INSA de Strasbourg, France) shared their data and knowledge to develop automated building damage detection (Rehor et al., 2008). Both studies presented algorithms for automatic plane detection from LiDAR point cloud data and the extracted plane surfaces were used as one important feature for building damage classification. The suitability of both algorithms for a more detailed building damage classification was analyzed, which led to promising outcome, and quantification of building damage using LiDAR data was revealed to be attractive.

#### 4.4. Optical and LiDAR data

Detection of building damage based on the combination of post-event optical imagery and LiDAR data for the rich texture information in optical images and the height information in LiDAR data is ideal. Rehor and Voegtle (2008) improved a previously proposed building damage detection and classification method (Rehor 2007) based on LiDAR data by combining it with optical data. The improved method considered the spectral characteristics of undamaged and damaged buildings from three different data types (laser intensity data, multi spectral scanner data, and high resolution digital orthophotos) and tested different texture parameters to select the features that could further enhance the results. Higher detection rate was obtained by using multi-spectral orthophotos as compared with that from only LiDAR data. Yu et al. (2010) extracted collapsed buildings through object-based image analysis and support vector machine (SVM) from aero-photographs and normalized DSM extracted from LiDAR data. In this study image segmentation using scale and homogeneity parameters (color, shape, and elevation value) was conducted firstly. Then, the greenness index and three different textural features derived from GLCM (Grey-Level Co-occurrence Matrix) were extracted from the brightness image. Finally, the collapsed buildings were detected with a SVM classifier. Hussain et al. (2011) used a GeoEye-1 image and LiDAR data to detect damaged buildings and debris for the city of Port-au-Prince after the Haiti earthquake. To handle the very complex urban structures of the city, the study was executed by performing an object-based one-class-at-a-time classification using spectral, textural, and height information. This method can be used to assess the volume of rubble and debris to prioritize the resources required for clearance.

**Table 4**

Summary of the studies using both pre- and post-earthquake data.

		Block level		Building level		
		Two grades	More than two grades	Two grades	Three grades	More than three grades
Optical data	Aerial	Ishii et al. (2002)		Gamba and Casciati (1998), Saito et al. (2004), Turker and Cetinkaya (2005), and Adams et al. (2005)	Rezaeian and Gruen (2007), Rezaeian (2010), Gerke and Kerle (2011), Tong et al. (2012)	Saito and Spence (2005)
	Satellite	Yusuf et al. (2001)	Turker and San (2003), Zhang et al. (2003), Huyck et al. (2005), Rathje et al. (2005b), and Kohiyama and Yamazaki (2005)	Sakamoto et al. (2004), Gusella et al. (2005), Li et al. (2009), and Chini et al. (2011)	Liu et al. (2004) and Gamba et al. (2007b)	Bitelli et al. (2004), Yamazaki et al. (2004), Yamazaki and Matsuoka (2007), Chesnel et al. (2007), Pesaresi et al. (2007), Iwasaki and Yamazaki (2011), and Bignami et al. (2011)
SAR data	Aerial Satellite	Yonezawa and Takeuchi (2001), Yonezawa et al. (2002), Ito et al. (2000), and Wang and Jin (2009)	Matsuoka and Yamazaki (2000, 2004, 2005, 2006), Hoffmann (2007), Arciniegas et al. (2007), Guida et al. (2010), Pan and Tang (2010)			
LiDAR data						Schweier et al. (2004), Schweier and Markus (2006), and Rehor (2007)
Optical & SAR data	Aerial Satellite		Stramondo et al. (2006), Chini et al. (2009), and Dell'Acqua et al. (2011)	Brunner et al. (2010), Uprety and Yamazaki (2012)	Dong et al. (2011)	Wang and Jin (2012)
Optical and ancillary data	Aerial Satellite		Turker and San (2003)			Samadzadegan and Rastiveisi (2008)
SSAR and ancillary data	Aerial Satellite		Gamba et al. (2007a), Trianni and Gamba (2008)	Liu et al. (2012)		

**Table 5**

Summary of the studies using only post-earthquake data.

		Block level		Building level		
		Two grades	More than two grades	Two grades	Three grades	More than three grades
Optical data	Aerial	Ishii et al. (2002) and Mitomi et al. (2002)	Duan et al. (2010)	Sirmacek and Unsalan (2009), Li et al. (2009), and Ma and Qin (2012)		Ogawa and Yamazaki (2000) and Rasika et al. (2006)
	Satellite	Vu et al. (2005) and Rathje et al. (2005a)	Yamazaki et al. (2007) and Liu et al. (2004)	Miura et al. (2007) and Vu and Ban (2010)		
SAR data	Aerial Satellite		Polli et al. (2010), Brunner et al. (2011), and Dell'Acqua and Polli (2011)			
LiDAR data						Rehor et al. (2008)
Optical and LiDAR data	Aerial			Yu et al. (2010)		Rehor and Voegtle (2008)
	Satellite			Hussain et al. (2011)		
Optical and ancillary data	Aerial			Guler and Turker (2004), Turker and San (2004), Turker and Sumer (2008), and Sumer and Turker (2006)		
	Satellite		Trianni and Gamba (2008)			

#### 4.5. Ancillary data

Damage to the buildings those disappear in post-event imagery can be identified with the help of a pre-event vector map of buildings. Methods using the combination of post-event optical imagery

and available ancillary data have also been proposed. Guler and Turker (2004) presented two approaches for detecting damaged buildings based on perceptual grouping and the relationship between a building and its shadow in post-event aerial imagery. Upon the perceptual grouping of line segments, each building

damage condition was assessed by measuring the agreement between the detected line segments and the available vector building boundaries. The overall and producer's accuracy were 72.6% and 79.7% respectively. However, the approach likely is unable to detect non-rectangular buildings, and the accuracy would decrease in heterogeneous areas. [Turker and San \(2004\)](#) introduced an earthquake-induced collapsed building detection approach deploying a digital analysis of post-event aerial photographs of the Izmit earthquake. This approach relies on the assumption that a collapsed building would not have a corresponding shadow. Building boundaries stored as vector polygons were used. The overall accuracy of this method was 96.15%, but it may not work in areas with complex-shape buildings or densely-packed buildings. Later, [Turker and Sumer \(2008\)](#) proposed an automated building damage detection approach using watershed segmentation of the post-event aerial images and the relationship between buildings and their shadows. In this method, vector building boundaries were used and the results at the building level were obtained. This approach was applied to the Izmit earthquake and yielded an overall accuracy of 80.6%. Using post-event panchromatic aerial imagery, [Sumer and Turker \(2006\)](#) proposed a building damage detection method based on gray-value and gradient orientation of the buildings and developed a corresponding building damage detection system. This method assumed that the gradient direction of collapsed buildings was randomly distributed as compared to that of non-collapsed buildings. About 90% of the buildings were labeled correctly as damaged or undamaged with this method.

## 5. Conclusion

To facilitate the reading, we summarize the reviewed studies in this paper into [Tables 4 and 5](#), which are respectively for the studies using both pre- and post-event data, and only post-event data. The two tables list the reported capabilities of the studies in identifying the grades of damaged blocks and buildings.

The in-depth analysis of a substantial number of building damage detection methods has demonstrated that they were designed in accordance with the characteristics of the applied data and the affected area in almost all cases. Thus, a quantitative comparative evaluation of all these methods is challenging because they cannot be tested with one or more sets of experimental data. Nonetheless, some conclusive remarks common to the recent developments and findings of most studies can be drawn from the above extensive review.

An increasingly large amount of diverse remote sensing and related GIS data are utilized in building damage detection. The remote sensors vary from airborne to spaceborne. The data types include optical, SAR, LiDAR, and vector maps. The resolution is also varying, from 10 to 0.3 m. Advantages of various data are made them useful for different scenarios and purposes. Most studies agree that data at a 10 m resolution can only identify damage at the block level, whereas the detection of individual damaged buildings requires a resolution at least 1 meter, with 0.5 m for a more reliable outcome.

Different types of remote sensing data show varying and sometimes complementary functionalities in building damage detection. A large amount of image archives makes optical imagery a valuable source for pre-event reference data. In addition, optical imagery can be easily interpreted to assist the first response to an earthquake, whereas SAR imagery can be acquired immediately after an earthquake independent to the weather conditions. The unique property of LiDAR data is its capability to detect building damage via evaluating its elevation changes or patterns, which is helpful to identify pancake type of collapse and estimate debris volume.

Diverse successful rates are reported for building damage detection. The range varies from about 70% to over 90%, depending on the availability and quality of the data. Usually a higher successful rate can be achieved when both pre and post-event data, especially multi-view data, are used. Whereas when only post-event data are available, the detection is usually limited to the block level unless VHR images of a resolution of 0.5 m or higher are involved. Ancillary data such as 2D building footprints or 3D building models can help locate buildings on images, detect damage, and determine damage grade with a higher reliability.

Visual interpretation remains to be the most reliable and independent evaluation for automated methods, especially for the determination of a lower damage grade. By visual interpretation, data from different sources and sensors can be precisely integrated, a task still being difficult for today's automated approaches. Most studies underwent this procedure for quality control. The results from visual interpretation are often used as the benchmark for validating the results from the automated methods.

Research efforts have been well split between using both pre- and post-event data, and only post-event data for building damage assessment. However, there seems to be a trend that slightly more attention has been paid to methods using only post-event data since 2008 when diverse and more VHR images become available. With the assistance of ancillary data, most of the automatic methods are able to detect building-level damage and distinguish three damage grades when using both pre- and post-event data. Conversely, the capability of post-event data alone is mostly at the block level, with some at the building level for separation of two damage grades. The performance of both efforts may be improved by a combined use of multiple data sources, especially the ancillary data. Among the reported studies, the use of optical images has been dominant, while SAR data are rapidly catching more attention because of its ever higher resolution.

Several future directions may be noted. Methods using LiDAR data should be studied further because their height information can identify more damage types and extract additional useful information like the volumes of rubble and debris. Use of optical and SAR data has a great potential for rapid building damage detection immediately after an earthquake. However, the few reported studies have not fully exploited the strengths of SAR and optical data because of their entirely different radiometric and physical properties. Limited studies using only SAR imagery at 1 m or coarser resolution are all at the block level, which suggests the need for further work with emerging higher resolution SAR data.

Effective and efficient collaboration among a larger community of experts in different fields has become important for reliable damage assessment, rapid decision making, and timely rescue operation. Remote sensing data with spatial resolutions of 1 m or finer are readily available for damage assessment through international organizations (e.g., The International Charter Space and Major Disasters) and governmental agencies (e.g., the Hazards Data Distribution System of the U.S. Geological Survey) ([Duda and Jones, 2011](#)). A crowdsourcing type of effort, through all stages of damage assessment, as demonstrated recently during the mitigation of the Haiti earthquake, may deserve further attention and collective effort.

## Acknowledgement

This work was partially supported by the National Basic Research Program of China under Grant 2012CB719904.

## References

- Adams, B.J., Mansouri, B., Huyck, C.K., 2005. Streamlining post-earthquake data collection and damage assessment for the 2003 Bam, Iran earthquake using

- visualizing impacts of earthquakes with satellites (VIEWS). *Earthquake Spectra* 21 (S1), 213–218.
- Arciniegas, G.A., Bijker, W., Kerle, N., Tolpekin, V.A., 2007. Coherence- and amplitude-based analysis of seismogenic damage in Bam, Iran, using ENVISAT ASAR data. *IEEE Transactions on Geoscience and Remote Sensing* 45 (6), 1571–1581.
- Balz, T., Liao, M.S., 2010. Building-damage detection using post-seismic high-resolution SAR satellite data. *International Journal of Remote Sensing* 31 (13), 3369–3391.
- Bartels, S.A., VanRooyen, M.J., 2011. Medical complications associated with earthquakes. *The Lancet* 379 (9817), 748–757.
- Benediktsson, J.A., Pesaresi, M., Arnason, K., 2003. Classification, feature extraction for remote sensing images from urban areas based on morphological transformations. *IEEE Transactions on Geoscience and Remote Sensing* 41 (9), 1940–1949.
- Bigname, C., Chini, M., Stramondo, S., Emery, W.J., Pierdicca, N., 2011. Objects textural features sensitivity for earthquake damage mapping. 2011 Joint Urban Remote Sensing Event (JURSE), 333–336.
- Bitelli, G., Camassi, R., Gusella, L., Mogno, A., 2004. Image change detection on urban areas: the earthquake case. *International Archive of Photogrammetry and Remote Sensing (IAPRS)* 35 (B7), 692–697.
- Brunner, D., Lemoine, G., Bruzzone, L., 2010. Earthquake damage assessment of buildings using VHR optical and SAR imagery. *IEEE Transactions on Geoscience and Remote Sensing* 48 (5), 2403–2420.
- Brunner, D., Schulz, K., Brehm, T., 2011. Building damage assessment in decimeter resolution SAR imagery A future perspective. 2011 Joint Urban Remote Sensing Event (Munich, Germany).
- Butenuth, M., Frey, D., Nielsen, A., Skriver, H., 2011. Infrastructure assessment for disaster management using multi-sensor and multi-temporal remote sensing imagery. *International Journal of Remote Sensing* 32, 8575–8594.
- Chesnel, A.L., Binet, R., Wald, L., 2007. Object oriented assessment of damage due to natural disaster using very high resolution images. In: *IEEE International Geoscience and Remote Sensing Symposium*, pp. 3736–3739.
- Chini, M., Bigname, C., Stramondo, S., Pierdicca, N., 2008. Uplift and subsidence due to the 26 December 2004 Indonesian earthquake detected by SAR data. *International Journal of Remote Sensing* 29 (13), 3891–3910.
- Chini, M., Cinti, F.R., Stramondo, S., 2011. Co-seismic surface effects from very high resolution panchromatic images: the case of the 2005 Kashmir (Pakistan) earthquake. *Natural Hazards and Earth Systems Science* 11 (3), 931–943.
- Chini, M., Pierdicca, N., Emery, W.J., 2009. Exploiting SAR and VHR optical images to quantify damage caused by the 2003 Bam earthquake. *IEEE Transactions on Geoscience and Remote Sensing* 47 (1), 145–152.
- Chini, M., Piscini, A., Cinti, F., Amici, S., Nappi, R., De Martini, P., 2013. The 2011 Tohoku (Japan) tsunami inundation and liquefaction investigated through optical, thermal, and SAR data. *IEEE Geoscience and Remote Sensing Letters* 10, 347–351.
- Chini, M., Pulvirenti, L., Pierdicca, N., 2012. Analysis and Interpretation of the COSMO-SkyMed Observations of the 2011 Japan Tsunami. *IEEE Geoscience and Remote Sensing Letters* 9, 467–471.
- Coppin, P., Jonckheere, I., Nackaerts, K., Muys, B., Lambin, E., 2004. Digital change detection methods in ecosystem monitoring: a review. *International Journal of Remote Sensing* 25 (9), 1565–1596.
- Corbane, C., Saito, K., Dell’Oro, L., Gill, S.P.D., Piard, B.E., Huyck, C.K., Kemper, D., Lemoine, G., Spence, R.J.S., Shankar, R., Senegas, O., Ghesquiere, F., Lallemand, T., Evans, G.B., Gartley, R.A., Toro, J., Ghosh, S., Svekla, W.D., Adams, B.J., Eguchi, R.T., 2011. A comprehensive analysis of building damage in the 12 January 2010 M(W)7 Haiti earthquake using high-resolution satellite- and aerial imagery. *Photogrammetric Engineering and Remote Sensing* 77, 997–1009.
- Cossu, R., Dell’Acqua, F., Polli, D.A., Rogolino, G., 2012. SAR-based seismic damage assessment in urban areas: scaling down resolution, scaling up computational performance. *IEEE Journal of Selected Topics in Applied Earth Observations and Remote Sensing* 5 (4), 1110–1117.
- Dell’Acqua, F., Bigname, C., Chini, M., Lisini, G., Polli, D.A., Stramondo, S., 2011. Earthquake damages rapid mapping by satellite remote sensing data: L’Aquila April 6th, 2009 Event. *IEEE Journal of Selected Topics in Applied Earth Observations and Remote Sensing* 4 (4), 935–943.
- Dell’Acqua, F., Polli, D.A., 2011. Post-event only VHR radar satellite data for automated damage assessment: a study on COSMO/SkyMed and the 2010 Haiti earthquake. *Photogrammetric Engineering and Remote Sensing* 77, 1037–1043.
- Dong, Y.F., Li, Q., Dou, A.X., Wang, X.Q., 2011. Extracting damages caused by the 2008 Ms 8.0 Wenchuan earthquake from SAR remote sensing data. *Journal of Asian Earth Sciences* 40 (4), 907–914.
- Duan, F.Z., Gong, H.L., Zhao, W.J., 2010. Collapsed houses automatic identification based on texture changes of post-earthquake aerial remote sensing image. In: 18th International Conference on Geoinformatics.
- Duda, K.A., Jones, B.K., 2011. USGS remote sensing coordination for the 2010 Haiti earthquake. *Photogrammetric Engineering and Remote Sensing* 77 (9), 899–907.
- Ehrlich, D., Guo, H.D., Molch, K., Ma, J.W., Pesaresi, M., 2009. Identifying damage caused by the 2008 Wenchuan earthquake from VHR remote sensing data. *International Journal of Digital Earth* 2 (4), 309–326.
- Fukuoka, T., Koshimura, S., 2011. Quantitative analysis of tsunami debris by object-based image classification of aerial photos. In: 9th International Workshop on Remote Sensing for Disaster Response.
- Gabriel, A.K., Goldstein, R.M., Zebker, H.A., 1989. Mapping small elevation change over large areas: differential radar interferometry. *Journal of Geophysical Research* 94 (B7), 9183–9191.
- Gamba, P., Casciati, F., 1998. GIS and image understanding for near-real-time earthquake damage assessment. *Photogrammetric Engineering and Remote Sensing* 64, 987–994.
- Gamba, P., Dell’Acqua, F., Trianni, G., 2007a. Rapid damage detection in the Bam area using multitemporal SAR and exploiting ancillary data. *IEEE Transactions on Geoscience and Remote Sensing* 45 (6), 1582–1589.
- Gamba, P., Dell’Acqua, F., Odasso, L., 2007b. Object-oriented building damage analysis in VHR optical satellite images of the 2004 tsunami over Kalutara, Sri Lanka. 2007 Joint Urban Remote Sensing Event, 1–5.
- Gerke, M., Kerle, N., 2011. Automatic structural seismic damage assessment with airborne oblique pictometry imagery. *Photogrammetric Engineering and Remote Sensing* 77 (9), 885–898.
- Grunthal, G., 1998. European macroseismic scale 1998. *Cahiers du Centre Europeen de Geodynamique et de Seismologie* 15, 1–99.
- Guida, R., Iodice, A., Riccio, D., 2010. Monitoring of collapsed built-up areas with high resolution SAR images. In: *IEEE International Geoscience and Remote Sensing Symposium*, pp. 2422–2425.
- Guler, M.A., Turker, M., 2004. Detection of the earthquake damaged buildings from post-event aerial photographs using perceptual grouping. *International Archives of Photogrammetry, Remote Sensing and Spatial Information Sciences*.
- Guo, H.D., Lu, L.L., Ma, J.W., Pesaresi, M., Yuan, F.Y., 2009. An improved automatic detection method for earthquake-collapsed buildings from ADS40 image. *Chinese Science Bulletin* 54 (18), 3303–3307.
- Gusella, L., Adams, B.J., Bitelli, G.C., Huyck, K., Mogno, A., 2005. Object-oriented image understanding and post-earthquake damage assessment for the 2003 Bam, Iran, earthquake. *Earthquake Spectra* 21 (S1), S225–S238.
- Haralick, R.M., Shanmugan, K., Dinstein, I., 1973. Texture features for image classification. *IEEE Transactions on Systems, Man, and Cybernetics* 3, 610–621.
- Hoffmann, J., 2007. Mapping damage during the Bam (Iran) earthquake using interferometric coherence. *International Journal of Remote Sensing* 28 (6), 1199–1216.
- Huang, X., Zhang, L., 2012. Morphological building/shadow index for building extraction from high-resolution imagery over urban areas. *IEEE Journal of Selected Topics in Applied Earth Observations and Remote Sensing* 5 (1), 161–172.
- Hussain, E., Ural, S., Kim, K., Fu, C.S., Shan, J., 2011. Building extraction and rubble mapping for city of Port-au-Prince post-2010 earthquake with GeoEye-1 imagery and Lidar data. *Photogrammetric Engineering and Remote Sensing* 77 (10), 1011–1023.
- Huyck, C.K., Adams, B.J., Cho, S., Chung, H.-C., Eguchi, R.T., 2005. Towards rapid citywide damage mapping using neighborhood edge dissimilarities in very high-resolution optical satellite imagery – application to the 2003 Bam, Iran earthquake. *Earthquake Spectra* 21 (S1), S255–S266.
- Irvin, R., Mckeown, D., 1989. Methods for exploiting the relationship between buildings and their shadows in aerial imagery. *IEEE Transactions on Systems, Man, and Cybernetics*, 19.
- Ishii, M., Goto, T., Sugiyama, T., Saji, H., Abe, K., 2002. Detection of earthquake damaged areas from aerial photographs by using color and edge information. In: 5th Asian Conference on Computer Vision, Melbourne, Australia.
- Ito, Y., Hosokawa, M., Lee, H., Liu, J.G., 2000. Extraction of damaged regions using SAR data and neural networks. In: *Proceeding of 19th International Society for Photogrammetry and Remote Sensing (ISPRS) Conference*, pp. 156–163.
- Iwasaki, Y., Yamazaki, F., 2011. Detection of building collapse from the shadow lengths in optical satellite images. In: 32nd Asian Conference on Remote Sensing, Taiwan, China.
- Joyce, K.E., Belliss, S.E., Samsonov, S.V., McNeill, S.J., Glassey, P.J., 2009. A review of the status of satellite remote sensing and image processing techniques for mapping natural hazards and disasters. *Progress in Physical Geography* 32 (2), 183–207.
- Kawai, A., 1995. Photo album: Buildings destructed in the great earthquake. *Dai-san-shokan*, pp. 1–207.
- Kaya, G., Musaoglu, N., Ersoy, O., 2011. Damage assessment of 2010 Haiti earthquake with post-earthquake satellite image by support vector selection and adaptation. *Photogrammetric Engineering and Remote Sensing* 77, 1025–1035.
- Kerle, N., 2010. Satellite-based damage mapping following the 2006 Indonesia earthquake – how accurate was it. *International Journal of Applied Earth Observation and Geoinformation* 12 (6), 466–476.
- Kohiyama, M., Yamazaki, F., 2005. Damage detection for 2003 Bam, Iran earthquake using Terra-ASTER satellite imagery. *Earthquake Spectra* 21 (S1), S267–S274.
- Li, P.J., Xu, H.Q., Liu, S.A., Guo, J.C., 2009. Urban building damage detection from very high resolution imagery using one-class SVM and spatial relations. In: *IEEE International Geoscience and Remote Sensing Symposium*, vol. 1–5, pp. 3537–3539.
- Li, X., Yang, W., Ao, T., Li, H., Chen, W., 2011. An improved approach of information extraction for earthquake-damaged buildings using high-resolution imagery. *Journal of Earthquake and Tsunami* 5, 389–399.
- Liu, J.H., Shan, X.J., Yin, J.Y., 2004. Automatic recognition of damaged town buildings caused by earthquake using remote sensing information: Taking the 2001 BHUJ, India Earthquake and the 1976 Tangshan, China Earthquake as examples. *Acta Seismologica Sinica* 26 (6), 623–632.

- Liu, W., F. Yamazaki, H. Gokou, S. Koshimura, 2012. Extraction of damaged buildings due to the 2011 Tohoku, Japan Earthquake Tsunami. IEEE International Geoscience and Remote Sensing Symposium, Melbourne, Australia.
- Liu, Y., Qu, C., Shan, X., Song, X., Zhan, G., Zhang, G., 2010. Application of SAR data to damage identification of the Wenchuan earthquake. *Acta Seismologica Sinica* 32 (2), 2142–2223.
- Ma, J., Qin, S., 2012. Automatic depicting algorithm of earthquake collapsed buildings with airborne high resolution image. In: IEEE International Geoscience and Remote Sensing Symposium, pp. 939–942.
- Malinverni, E.S., 2011. Change detection applying landscape metrics on high remote sensing images. *Photogrammetric Engineering and Remote Sensing* 77 (10), 1045–1056.
- Mansouri, B., Shinozuka, M., Nourjou, R., 2007. SAR remote sensing for urban damage assessment for Tehran. In: 5th International Workshop Remote Sensing Application Natural Hazards Proceedings. Washington, DC, America.
- Mas, J.F., 1999. Monitoring land-cover changes: a comparison of change detection techniques. *International Journal of Remote Sensing* 20 (1), 139–152.
- Massonnet, D., Rossi, M., Carmona, C., Adragna, F., Peltzer, G., Feigl, K., Rabaute, T., 1993. The displacement field of the Landers earthquake mapped by radar interferometry. *Nature* 364, 138–142.
- Matsuoka, M., Yamazaki, F., 1999. Characteristics of satellite images of damaged areas due to the 1995 Kobe earthquake. In: 2nd Conference on the Applications of Remote Sensing and GIS for Disaster Management.
- Matsuoka, M., Yamazaki, F., 2000. Use of interferometric satellite SAR for earthquake damage detection. In: Proceedings of 6th International Conference of Seismic Zonation, pp. 103–108.
- Matsuoka, M., Yamazaki, F., 2004. Use of satellite SAR intensity imagery for detecting building areas damaged due to earthquakes. *Earthquake Spectra* 20 (3), 975–994.
- Matsuoka, M., Yamazaki, F., 2005. Building damage mapping of the 2003 Bam, Iran Earthquake using Envisat/ASAR intensity imagery. *Earthquake Spectra* 21 (S1), S285–S294.
- Matsuoka, M., Yamazaki, F., 2006. Use of SAR imagery for monitoring areas damaged due to the 2006 Mid Java, Indonesia Earthquake. In: Proceedings of 4th International workshop on Remote Sensing for Post-Disaster Response, Cambridge, United Kingdom.
- Mercier, G., Moser, G., Serpico, S.B., 2008. Conditional copulas for change detection in heterogeneous remote sensing images. *IEEE Transactions on Geoscience and Remote Sensing* 46 (5), 1428–1441.
- Mitomi, H., Matsuoka, M., Yamazaki, F., 2002. Application of automated damage detection of buildings due to earthquakes by panchromatic television images. In: Proceedings of Seventh U.S. National Conference on Earthquake Engineering. EERI, USA, CD-ROM, p. 10.
- Miura, H., Modorikawa, S., Chen, S.H., 2011. Texture characteristics of high-resolution satellite images in damaged areas of the 2010 Haiti Earthquake. In: Proceedings of 9th International Workshop on Remote Sensing for Disaster Response, pp. 1–9.
- Miura, H., Yamazaki, F., Matsuoka, M., 2007. Identification of damaged areas due to the 2006 Central Java, Indonesia Earthquake using satellite optical images. In: Proceedings of Urban Remote Sensing Joint Event, Paris, France.
- Ogawa, N., Yamazaki, F., 2000. Photo-Interpretation of building damage due to earthquakes using aerial photographs. In: 12th World Conference on Earthquake Engineering. Auckland, New Zealand.
- Okada, S., Takai, N., 2000. Classifications of structural types and damage patterns of buildings for earthquake field investigation. In: 12th World Conference on Earthquake Engineering. Auckland, New Zealand.
- Ouzounov, D., Bryant, N., Logan, T., Pulinets, S., Taylor, P., 2006. Satellite thermal IR phenomena associated with some of the major earthquakes in 1999–2003. *Physics and Chemistry of the Earth* 31 (4–9), 154–163.
- Pan, G., Tang, D.L., 2010. Damage information derived from multi-sensor data of the Wenchuan Earthquake of May 2008. *International Journal of Remote Sensing* 31, 3509–3519.
- Pesaresi, M., Benediktsson, J.A., 2001. A new approach for the morphological segmentation of high-resolution satellite imagery. *IEEE Transactions on Geoscience and Remote Sensing* 39 (2), 309–320.
- Pesaresi, M., Gerhardinger, A., Haag, F., 2007. Rapid damage assessment of built-up structures using VHR satellite data in tsunami-affected areas. *International Journal of Remote Sensing* 28 (13/14), 3013–3036.
- Polli, D., Dell'Acqua, F., Gamba, P., Lisini, G., 2010. Earthquake damage assessment from post-event only radar satellite data. In: Proceedings 8th International Workshop on Remote Sensing for Disaster Management, p. 30.
- Rasika, A.K., Kerle, N., Heuel, S.R.K.B., 2006. Multi-scale texture and color segmentation of oblique airborne video data for damage classification. *ISPRS mid-term symposium remote sensing: from pixels to processes*.
- Rathje, E.M., Crawford, M., Woo, K., Neuenschwander, A., 2005a. Damage patterns from satellite images of the 2003 Bam, Iran, Earthquake. *Earthquake Spectra* 21 (1), 295–307.
- Rathje, E.M., Woo, K.S., Crawford, M., Neuenschwander, A., 2005b. Earthquake damage identification using multi-temporal high-resolution optical satellite imagery. In: IEEE International Geoscience and Remote Sensing Symposium, vol. 7, pp. 5045–5048.
- Rehor, M., 2007. Classification of building damages based on laser scanning data. *The International Archives of the Photogrammetry, Remote Sensing and Spatial Information Sciences* 36 (3/W52), 326–331.
- Rehor, M., Bahr, H.P., Tarsha-Kurdi, F., Landes, T., Grussenmeyer, P., 2008. Contribution of two plane detection algorithms to recognition of intact and damaged buildings in LiDAR data. *Photogrammetric Record* 23 (124), 441–456.
- Rehor, M., Voegtli, T., 2008. Improvement of building damage detection and classification based on laser scanning data by integrating spectral information. In: *The International Archives of the Photogrammetry, Remote Sensing and Spatial Information Sciences*, Beijing.
- Rezaeian, M., 2010. Assessment of earthquake damages by image-based techniques. *Electrical Engineering Doctor of Sciences* (19178), 149.
- Rezaeian, M., Gruen, A., 2007. Automatic classification of collapsed buildings using object and image space features. Springer: *Geomatics Solutions for Disaster Management*, 135–148.
- Saito, K., Spence, R.J., Going, C., Markus, M., 2004. Using high-resolution satellite images for post-earthquake building damage assessment: a study following the 26 January 2001 Gujarat earthquake. *Earthquake Spectra* 20 (1), 145–170.
- Saito, K., Spence, R.J.S., 2005. Visual damage assessment using high-resolution satellite images following the 2003 Bam, Iran, earthquake. *Earthquake Spectra* 21 (S1), S309–S318.
- Sakamoto, M., Takasago, Y., Uto, K., Kakumoto, S., Kosugi, Y., Doihara, T., 2004. Automatic detection of damaged area of Iran earthquake by high-resolution satellite imagery. In: IEEE International Geoscience and Remote Sensing Symposium, vol. 2, pp. 1418–1421.
- Samadzadegan, F., Rastiveisi, H., 2008. Automatic detection and classification of damaged buildings, using high resolution satellite imagery and vector data. *International Archives of Photogrammetry Remote Sensing and Spatial Information Sciences* 37 (B8), 415–420.
- Satake, M., Kobayashi, T., Uemoto, J., Umehara, T., Kojima, S., Matsuoka, T., Nadai, A., Uratsuka, S., 2012. Damage estimation of the Great East Japan Earthquake with airborne SAR (Pi-SAR2) data. In: IEEE International Geoscience and Remote Sensing Symposium, pp. 1190–1191.
- Schweier, C., Markus, M., 2006. Classification of collapsed buildings for fast damage and loss assessment. *Bulletin of Earthquake Engineering* 4, 177–192.
- Schweier, C., Markus, M., Steinle, E., 2004. Simulation of earthquake-caused building damages for the development of fast reconnaissance techniques. *Natural Hazards and Earth System Sciences* 4 (2), 285–293.
- Shinozuka, M., Loh, K., 2004. Remote sensing with the synthetic aperture radar (SAR) for urban damage detection. In: 9th International Conference Engineering, Construction, Operations in Challenging Environments, vol. 153, pp. 223–230.
- Sirmacek, B., Unsalan, C., 2009. Damaged building detection in aerial images using shadow information. In: Proceedings of the 4th International Conference on Recent Advances in Space Technologies, pp. 249–252.
- Stramondo, S., Bignami, C., Chini, M., Pierdicca, N., Tertulliani, A., 2006. Satellite radar and optical remote sensing for earthquake damage detection: results from different case studies. *International Journal of Remote Sensing* 27 (20), 4433–4447.
- Stramondo, S., Chini, M., Salvi, S., Bignami, C., Zoffoli, S., Boschi, E., 2008. Ground Deformation Imagery of the May Sichuan Earthquake. *EOS Transaction American Geophysical Union* 89, 341–342.
- Sumer, E., Turker, M., 2006. An integrated earthquake damage detection system. *The International Archives of the Photogrammetry, Remote Sensing and Spatial Information Sciences* 36 (4/C42), 6.
- Tomowski, D., Klonus, S., Ehlers, M., Michel, U., Reinartz, P., 2010. Change visualization through a texture-based analysis approach for disaster applications. In: *ISPRS Technical Commission VII Symposium – 100 Years ISPRS Advancing Remote Sensing Science Sensing Proceedings*, vol. 35, pp. 263–268.
- Tong, X., Hong, Z., Liu, S., Zhang, X., Xie, H., Li, Z., Yang, S., Wang, W., Bao, F., 2012. Building-damage detection using pre- and post-seismic high-resolution satellite stereo imagery: a case study of the May 2008 Wenchuan earthquake. *ISPRS Journal of Photogrammetry and Remote Sensing* 68, 13–17.
- Trianni, G., Gamba, P., 2008. Damage detection from SAR imagery: application to the 2003 Algeria and 2007 Peru earthquakes. *International Journal of Navigation and Observation*, 1–8.
- Tronin, A.A., Hayakawa, M., Molchanov, O.A., 2002. Thermal IR satellite data application for earthquake research in Japan and China. *Journal of Geodynamics* 33 (4–5), 519–534.
- Turker, M., Cetinkaya, B., 2005. Automatic detection of earthquake-damaged buildings using DEMs created from pre- and post-earthquake stereo aerial photographs. *International Journal of Remote Sensing* 26 (4), 823–832.
- Turker, M., San, B.T., 2003. SPOT HRV data analysis for detecting earthquake-induced changes in Izmit, Turkey. *International Journal of Remote Sensing* 24 (12), 2439–2450.
- Turker, M., San, B.T., 2004. Detection of collapsed buildings caused by the 1999 Izmit, Turkey earthquake through digital analysis of post-event aerial photographs. *International Journal of Remote Sensing* 25 (21), 4701–4714.
- Turker, M., Sumer, E., 2008. Building-based damage detection due to earthquake using the watershed segmentation of the post-event aerial images. *International Journal of Remote Sensing* 29 (11), 3073–3089.
- Tzeng, Y.C., Chiu, S.H., Chen, D., Chen, K.S., 2007. Change detections from sar images for damage estimation based on a spatial chaotic model. In: IEEE International Geoscience and Remote Sensing Symposium, pp. 1926–1930.
- Upreti, P., Yamazaki, F., 2012. Use of high-resolution SAR intensity images for damage detection from the 2010 Haiti Earthquake. In: IEEE International Geoscience and Remote Sensing Symposium, Melbourne, Australia.

- Voigt, S., Kemper, T., Riedlinger, T., Kiefl, R., Scholte, K., Mehl, H., 2007. Satellite image analysis for disaster and crisis-management support. *IEEE Transactions on Geoscience and Remote Sensing* 45 (6), 1520–1528.
- Vu, T.T., Ban, Y., 2010. Context-based mapping of damaged buildings from high-resolution optical satellite images. *International Journal of Remote Sensing* 31 (13), 3411–3425.
- Vu, T.T., Matsuoka, M., Yamazaki, F., 2004. Shadow analysis in assisting damage detection due to earthquakes from Quickbird imagery. *International Archives of Photogrammetry Remote Sensing and Spatial Information Sciences* 35 (7), 607–610.
- Vu, T.T., Matsuoka, M., Yamazaki, F., 2005. Detection and animation of damage using very high-resolution satellite data following the 2003 Bam, Iran earthquake. *Earthquake Spectra* 21 (S1), S319–S327.
- Wang, C., Zhang, H., Wu, F., Zhang, B., Tang, Y., Wu, H., Wen, X., Yan, D., 2009. Disaster phenomena of Wenchuan earthquake in high resolution airborne synthetic aperture radar images. *Journal of Applied Remote Sensing*, 3.
- Wang, H., Jin, Y.Q., 2009. Statistical analysis to assess building damage in 2008 Wenchuan earthquake from multi-temporal SAR images. In: 2nd Asian-Pacific Conference on Synthetic Aperture Radar, pp. 121–123.
- Wang, T.L., Jin, Y.Q., 2012. Post-earthquake building damage assessment using multi-mutual information from pre-event optical image and postevent SAR image. *IEEE Geoscience and Remote Sensing Letters* 9 (3), 452–456.
- Yamazaki, F., Kouchi, K., Matsuoka, M., Kohiyama, M., Muraoka, N., 2004. Damage detection from high-resolution satellite images for the 2003 Boumerdes, Algeria earthquake. In: 13th World Conference on Earthquake Engineering Vancouver: Paper No. 2595.
- Yamazaki, F., Matsuoka, M., 2007. Remote sensing technologies in post-disaster damage assessment. *Journal of Earthquake and Tsunami* 1 (3), 193–210.
- Yamazaki, F., Suzuki, D., Maruyama, Y., 2008. Detection of damages due to earthquakes using digital aerial images. In: 6th International Workshop on Remote Sensing for Disaster Applications Pavia, Italy.
- Yamazaki, F., Vu, T.T., Matsuoka, M., 2007. Context-based detection of post-disaster damaged buildings in urban areas from satellite images. In: Urban Remote Sensing Joint Event, Paris, France.
- Yamazaki, F., Yano, M., Matsuoka, M., 2005. Visual damage interpretation of buildings in Bam city using QuickBird images following the 2003 Bam, Iran earthquake. *Earthquake Spectra*, 21(S1): 329–336.
- Yonezawa, C., Takeuchi, S., 2001. Decorrelation of SAR data by urban damages caused by the 1995 Hyogoken-Nambu earthquake. *International Journal of Remote Sensing* 22 (8), 1585–1600.
- Yonezawa, C., Tomiyama, N., Takeuchi, S., 2002. Urban damage detection using decorrelation of SAR interferometric data. In: IEEE International Geoscience and Remote Sensing Symposium and 24th Canadian Symposium on Remote Sensing, Vols. I–VI, Proceedings, pp. 2051–2053.
- Yu, H., Cheng, G., Ge, X., 2010. Earthquake-collapsed building extraction from LiDAR and aerophotograph based on OBIA. In: 2nd International Conference on Information Science and Engineering (ICISE), pp. 2034–2037.
- Yusuf, Y., Matsuoka, M., Yamazaki, F., 2001. Damage assessment after 2001 Gujarat earthquake using Landsat-7 satellite images. *Journal of the Indian Society of Remote Sensing* 29 (1), 233–239.
- Zhang, J.F., Xie, L.L., Tao, X.X., 2003. Change detection of remote sensing image for earthquake damaged buildings and its application in seismic disaster assessment. In: Proceedings of 2003 IEEE International Geoscience and Remote Sensing Symposium, vol. 4, pp. 2436–2438.